and hence π is a square root of the involution $\hat{\kappa} = (2\ 10)\ (3\ 9)\ (4\ 8)\ (5\ 7)$. Therefore π must consist of 4-cycles. Since π preserves parity mod 2, like any dissipative meander, the 4-cycles must permute the sets $\{2, 4, 8, 10\}$ and $\{3, 5, 7, 9\}$, separately. Since (3.10) holds for the entire substitution orbit π^{-1}, $\kappa\pi\kappa$, $\kappa\pi^{-1}\kappa$, once it holds for π itself, only the two candidates $\pi = (2\ 8\ 10\ 4)\ (3\ 7\ 9\ 5)$ and $(2\ 8\ 10\ 4)\ (3\ 5\ 9\ 7)$ remain, without loss of generality. Since $(2\ 8\ 10\ 4)\ (3\ 5\ 9\ 7)$ is not a meander permutation, this proves

$$\pi = (2\ 8\ 10\ 4)\ (3\ 7\ 9\ 5), \tag{3.11}$$

to be the only self-dual case with $N = 11$ equilibria, up to trivial substitutions.
Motivated by the pitchforkable Chafee-Infante nonlinearity $f = \lambda u(1 - u^2)$, as discussed in [He85], [CoSm83], the self-dual case $11.3^2 - 3$ has already been considered in [Ro91] as an example of a non-pitchforkable Sturm attractor: *pitchforkable* attractors can be simplified by a pitchfork bifurcation which reduces the number of equilibria by 2. In terms of the Sturm permutation π, they feature three adjacent entries:

$$\begin{array}{lll} \pi = & (\ldots m-1 & m \quad m+1 \ldots) \quad \text{or} \\ \pi = & (\ldots m+1 & m \quad m-1 \ldots). \end{array} \tag{3.12}$$

By tables 3.1, 3.2 and their simpler ancestors with $N = 3, 5, 7$ and 9 equilibria, the self-dual attractor $11.3^2 - 3$ is in fact the first and lowest-dimensional non-pitchforkable example with up to 11 equilibria.

4 Specifics: the planar Platonic graphs

In sections 4.1–4.5 we design Sturm attractors with the five planar Platonic graphs G as 1-skeletons $\mathcal{C}_f^1$ of their connection graphs. Throughout we eliminate cases with substitution equivalent attractors or orientation isomorphic 1-skeletons G.
Polarity is a primary feature of Sturm attractors and, more generally, of any Morse system. This is caused by the two possible signs of any eigenfunction for any simple real eigenvalue and, consequently, by the two asymptotic directions of any trajectory which converges to any hyperbolic equilibrium – be it forward or backward in time, at a slower or faster exponential rate. See for example [BrFi86].
Such polarity is not easily accomodated by Platonic polyhedra. In the following sections we therefore present our attempts at designing planar Sturm attractors $\mathcal{A}_f$ such that the 1-skeletons $\mathcal{C}_f^1$ of their connection graphs coincide with the five Platonic graphs. Each of these planar graphs possesses only one plane embedding G, up to isomorphism, by the symmetries of the Platonic solids.

Case	Sturm permutation
π	1 12 11 4 5 10 9 6 3 2 7 8 13
$\kappa\pi^{-1}\kappa$	1 12 11 8 7 2 3 6 9 10 5 4 13

Table 4.1: Sturm permutations with the filled plane tetrahedral graph as connection graph.

Our general strategy follows theorems 1.1 and 1.2 via the recipe at the end of section 2.1. We first study inequivalent positions for the extreme equilibria $\underline{v}$ and $\bar{v}$ on G. We then enumerate the resulting admissible orientations of G, in the sense of theorem 1.1. Throughout section 3, the orientation was determined uniquely by the positions of $\underline{v}$ and $\bar{v}$, up to trivial substitutions. We will now see how the same geometric configuration of $\underline{v}$, $\bar{v}$ can accommodate several orientations. As was mentioned in sections 1 and 2.1, any admissible orientation then determines a unique boundary (ZS)-Hamiltonian pair (h_0, h_1) of paths from $\underline{v}$ to $\bar{v}$. This pair, in turn, defines the Sturm permutation $\pi = h_0^{-1}h_1$ which produces the prescribed Platonic connection graph with 1-skeleton $\mathcal{C}_f^1 = G$. Conversely, again by theorems 1.1, 1.2, any connection graph with $\mathcal{C}_f^1 = G$ defines an admissible orientation of G, and therefore must come from one of the Sturm permutations π which we have constructed.

4.1 The plane tetrahedral graph

See figure 4.1, left for the planar tetrahedral graph, the numbering of its vertices, and the two admissible orientations of its 1-skeleton. We only need to consider extremal vertices $\underline{v} = 1$ and $\bar{v} = 2$, possibly after rotation and interchange of $\underline{v}, \bar{v}$ by reflection σ_1 through the symmetry axis 35 of the plane embedded tetrahedral graph.
The two admissible orientations on the 1-skeleton G are related as follows. Reflecting through 35 and reversing all arrows transforms one orientation into the other. Consequently, the right diagram of figure 4.1 is obtained from the center diagram by reflection through 35, reversal of all arrows, and interchange of h_0, h_1.
To derive the associate Sturm permutations $\pi = \pi_f$ which turn figure 4.1 into an attractor design, we recall $\pi = h_0^{-1} \circ h_1$ from (2.3). Relabeling vertices does not affect π. Let us therefore relabel vertices such that the Z-Hamiltonian path $h_0 = id$: we simply tag vertices along the path h_0. Then $\pi = h_1$ simply collects the same tags along the S-Hamiltonian path h_1; see (2.4).
The Sturm permutations π_1, π_2 leading to – or generated by – the center and right diagrams in figure 4.1 are given explictly in table 4.1. Note that $\pi_2 = \kappa\pi^{-1}\kappa$ is trivially substitution equivalent to π_1 by symmetry σ_1. Neither permutation is pitchforkable. Inspection of the duals G^*, as in section 3, shows that the tetrahedral graphs are face-glued versions of the

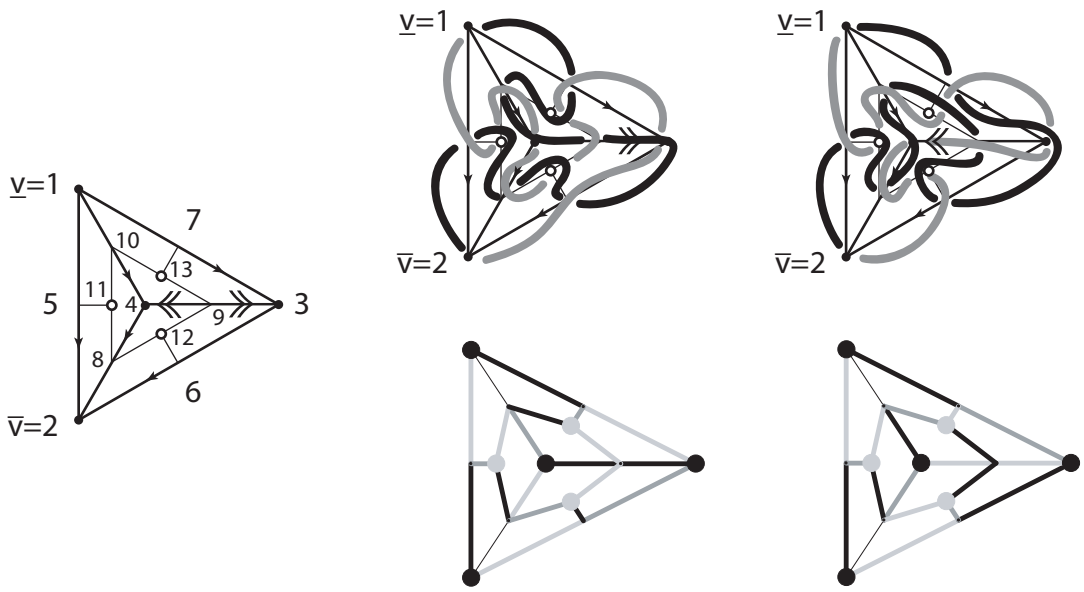

Figure 4.1: The filled plane tetrahedral graph. Left: numbering of vertices and orientations. Center and right: boundary ZS-Hamiltonian pairs (h_0, h_1). Double arrows indicate deviating orientations. Top row: disentangled paths h_0 (black) and h_1 (gray). Simplified diagrams in bottom row: edges traversed by both h_0 and h_1 are gray; black is for h_0, and light gray for h_1, alone; thin edges for neither.

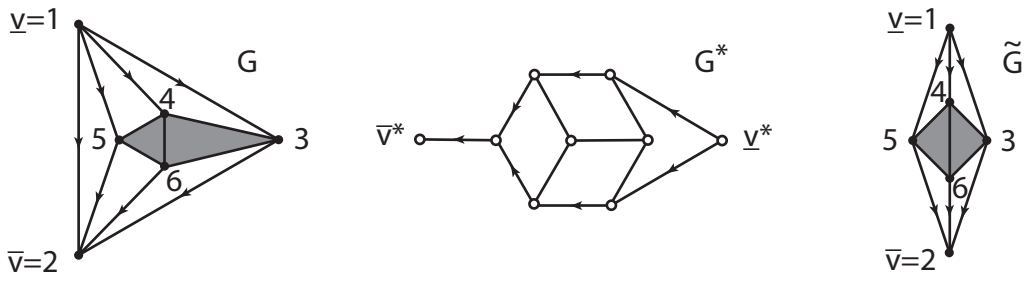

Figure 4.2: The plane octahedral graph G. Left: numbering of vertices and basic orientations. Center: the dual 1-skeleton G^*. Right: G after removal of glued triangle 125 on the left.

self-dual case $11.3^2 - 3$; see also figure 3.11 and table 3.2. The gluing face is the triangle 124 in G. Face gluing always applies, trivially, for adjacent extrema $\underline{v}$, $\bar{v}$ on ∂G.

4.2 The plane octahedral graph

See figure 4.2, left, for the plane octahedral graph G, the numbering of its vertices, and the basic orientation constraints induced by the extremal vertices $\underline{v}$ and $\bar{v}$. Again we only need to consider adjacent extremal vertices $\underline{v} = 1$ and $\bar{v} = 2$, without loss of generality.
Before we determine all remaining possibilities for the orientations in the "square" 3456, we trivially observe that the face 125 is a gluing face; see the stacking in the dual, figure 4.2, center. We are therefore left with the orientation problem of the reduced graph $\tilde{G}$ on the right of figure 4.3. More precisely, we have to check the 2^5 possible orientations of the five edges in the square 3456 for their admissibility.
Instead of case-by-case, we proceed by isotropy with respect to the symmetries of the reduced 1-skeleton $\tilde{G}$. Let σ_1 denote reflection of G through the horizontal axis 35, again, which comes with reversal of all orientation arrows. To fix $\underline{v}$, $\bar{v}$, we also reverse and interchange the ZS-Hamiltonian paths h_0, h_1 from $\underline{v}$ to $\bar{v}$. Let σ_2 denote the reflection of $\tilde{G}$ through the vertical axis $\underline{v}\ \bar{v} = 12$, which also interchanges h_0, h_1 but does not reverse arrows. Rotation by 180°, with orientation reversal, is the composite $\sigma_1\sigma_2$ of the commuting reflections. The orientation of the edge $\{4, 6\}$ in the square 3456 is affected by neither of these automorphism of the (unoriented) graph $\tilde{G}$. Let I denote the *orientation isotropy* of $\tilde{G}$, that is the subgroup of those elements in the symmetry group $\Gamma = \langle \sigma_1, \sigma_2 \rangle = \{id, \sigma_1, \sigma_2, \sigma_1\sigma_2\}$ of $\tilde{G}$ which also respect a given orientation of $\tilde{G}$.
First suppose $\sigma_1 \in I$. Then the edges {4,5} and {5,6} possess antiparallel orientation, as do

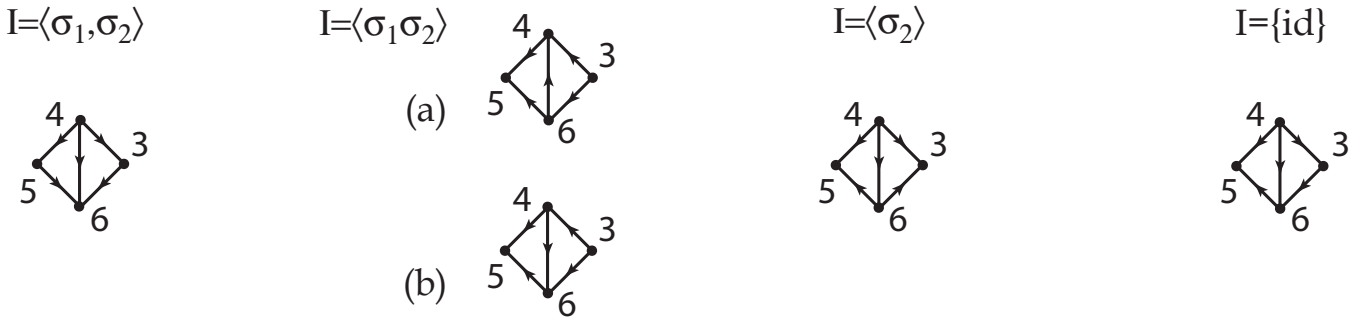

Figure 4.3: Orientations and isotropies I of the octahedral square 3456, up to action by $\Gamma = \langle \sigma_1, \sigma_2 \rangle$.

Isotropy I	Sturm permutation
$\Gamma = \langle \sigma_1, \sigma_2 \rangle$	1 24 23 16 15 4 5 14 17 22 21 18 13 12 11 6 3 2 7 10 19 20 9 8 25
$\langle \sigma_2 \rangle$	1 24 23 20 19 4 5 18 17 8 9 16 21 22 15 14 13 10 7 6 3 2 11 12 25
$\langle \sigma_1, \sigma_2 \rangle$, (a)	1 24 23 20 19 16 15 2 3 14 13 6 7 12 17 18 11 10 21 22 9 8 5 4 25
$\langle \sigma_1 \sigma_2 \rangle$, (b)	1 24 23 20 19 10 9 2 3 8 11 18 17 12 7 6 13 16 21 22 15 14 5 4 25
$\{id\}$, (a)	1 24 23 20 19 4 5 18 17 12 11 6 3 2 7 10 13 16 21 22 15 14 9 8 25
$\{id\}$, (b)	1 24 23 12 11 4 5 10 13 22 21 14 9 8 15 20 19 16 7 6 3 2 17 18 25

Table 4.2: Sturm permutations π with the filled plane octahedral graph as connection graph. Substitution equivalent and orientation isomorphic copies are omitted. See also figure 4.4

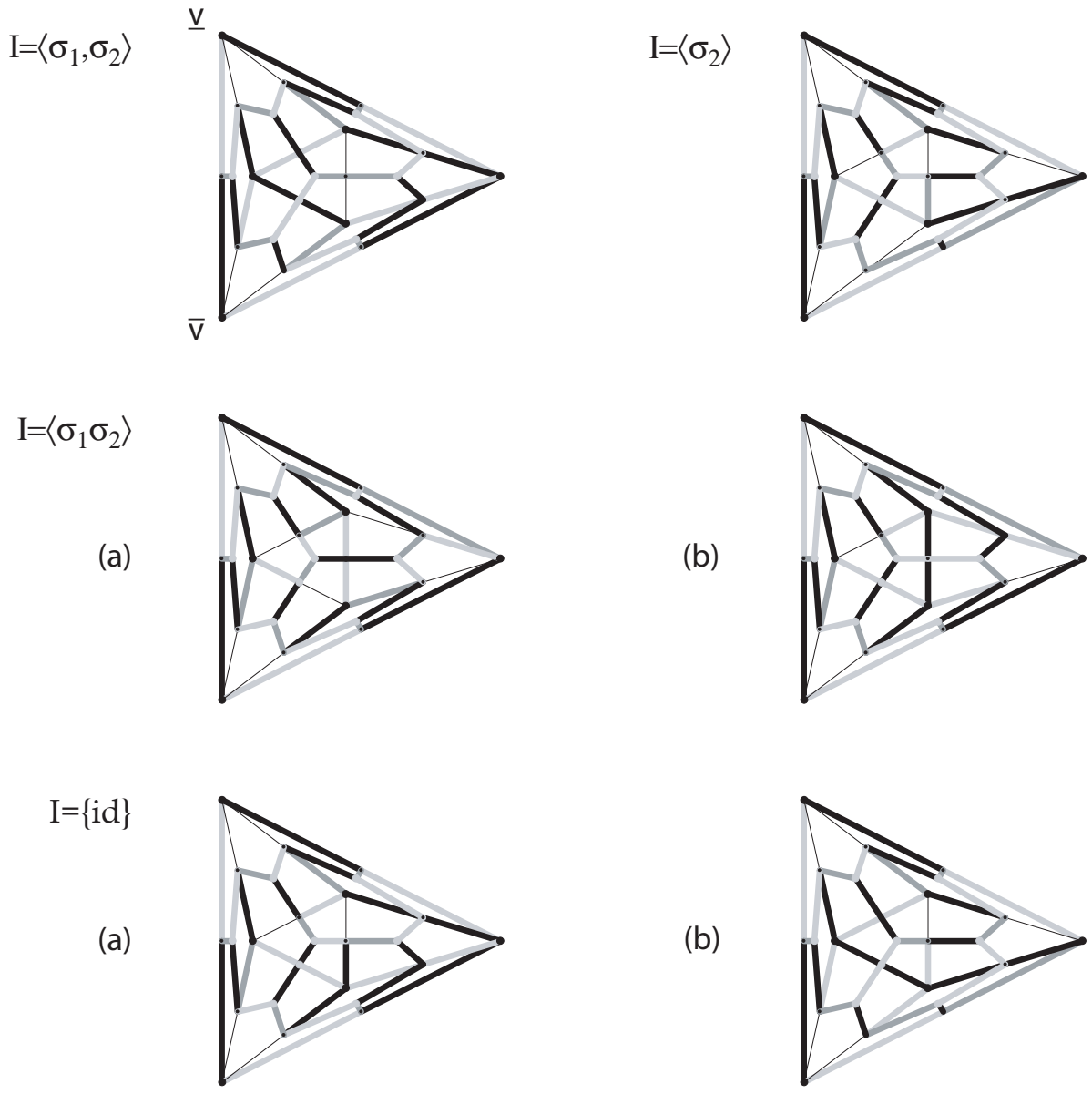

Figure 4.4: The six boundary ZS-Hamiltonian pairs (h_0, h_1) for the planar octahedral graph. For Sturm permutations and enumeration of cases by isotropy I see table 4.2. Edges traversed by both h_0 and h_1 are gray; black is for h_0, light gray for h_1 alone; thin edges for neither.

{3,4} and {3,6}. Because none of the vertices 3,5 is di-critical in G, in the sense of section 1, the resulting orientations are 45, 56, and 43, 36. Acyclicity of the orientation then implies downward orientation 46 of the vertical diagonal edge {4,6}. This unique case therefore possesses full isotropy, $I = \Gamma = \langle \sigma_1, \sigma_2 \rangle$. See figure 4.3
Next suppose $\sigma_1 \notin \Gamma$. Then at least one of the above two nonvertical edge pairs must possess parallel orientation. Acting by σ_2, we may assume the left pair {4,5}, {5,6} to be parallel. Acting by σ_1 we may assume outward orientation 45, 65. Two cases arise here:

(a) upward orientation 64 of the vertical edge. Because neither vertex 4 nor vertex 6 is di-critical, this implies the orientations 34 and 36, with resulting isotropy $I = \langle \sigma_1, \sigma_2 \rangle$. See figure 4.3, $I = \langle \sigma_1 \sigma_2 \rangle$, case (a).

(b) downward orientation 46 of the vertical edge. If $\sigma_1 \sigma_2 \in I$, i.e., $I = \langle \sigma_1 \sigma_2 \rangle$, then 45, 65 imply 36, 34, respectively. See figure 4.3, $I = \langle \sigma_1 \sigma_2 \rangle$, case (b).

If $\sigma_2 \in I_2$, i.e., $I_2 = \langle \sigma_2 \rangle$, then we obtain 63, 43, instead, as in figure 4.3, $I = \langle \sigma_2 \rangle$.
Finally, therefore, trivial isotropy comes with antiparallel orientation of the edges {3,4} and {3,6}. Because vertex 3 is not di-critical in G, this implies 43, 36, as in figure 4.3, $I = \{id\}$.
The five cases of figure 4.3 therefore exhaust all admissible orientations of the reduced square 3456 in the reduced 1-skeleton $\tilde{G}$ and in the octahedral 1-skeleton G, alike. For the associated boundary ZS-Hamiltonian pairs from $\underline{v} = 1$ to $\bar{v} = 2$ see figure 4.4. As in the case of the tetrahedron, we may relabel vertices such that $h_0 = id$. Then the Sturm permutations $\pi = \pi_f$ are given by the paths h_1 as $\pi = h_1$. In table 4.2 we list the resulting six Sturm permutations. We omit the trivial substitution action of σ_1, given by $\pi \mapsto \kappa \pi^{-1} \kappa$. Only for trivial isotropy, $I = \{id\}$, the actions of the remaining group elements cannot be represented by σ_1 alone. Instead, we obtain two permutations, which are related by σ_2, in this case. Only the case with isotropy $I = \langle \sigma_2 \rangle$ is pitchforkable. In figure 4.4 it is informative to check the isotropies I with respect to σ_1, on G_2, and with respect to σ_2, on the filled reduced graph $\tilde{G}_2$ of $\tilde{G}$, in terms of reflections, orientation reversals, and interchanges of h_0, h_1.

4.3 The plane hexahedral (cube) graph

See figure 4.5, left, for the plane hexahedral graph G, otherwise known as the 1-skeleton of the 3-cube. Immediately two cases arise, depending on the relative position of the extrema $\underline{v}$, $\bar{v}$. Indeed, $\underline{v}$ and $\bar{v}$ may either be adjacent, or else diagonally opposite on the boundary ∂G.

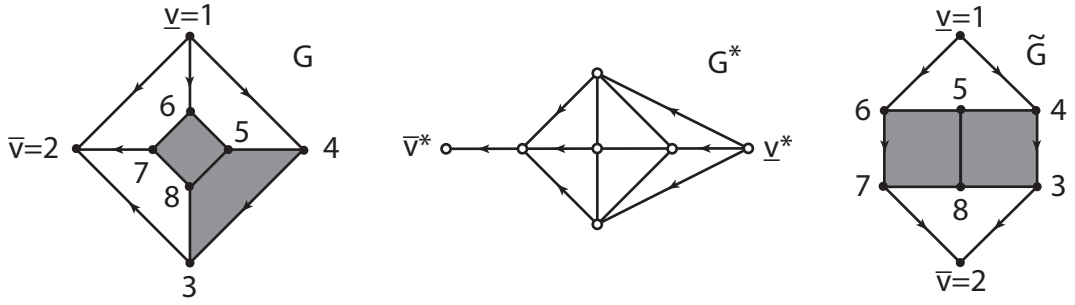

Figure 4.5: The plane hexahedral graph G with adjacent extrema $\underline{v} = 1$, $\bar{v} = 2$. Left: numbering of vertices and basic orientations. Center: dual 1-skeleton G^*. Right: reduced 1-skeleton $\tilde{G}$ after removal of the glued trapezoid 1276 from G.

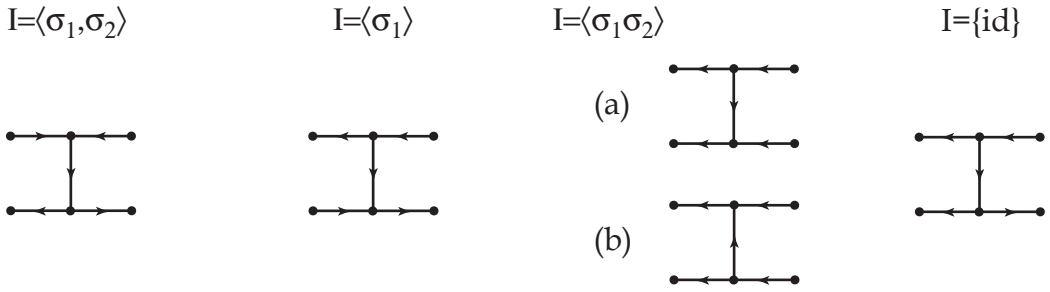

Figure 4.6: Orientations and isotropies of the hexahedral "letter I" spanned by the vertices 345678.

Isotropy I	Sturm Permutation
$\Gamma = \langle \sigma_1, \sigma_2 \rangle$	1 24 23 8 9 20 19 10 7 2 3 6 11 12 13 18 21 22 17 14 5 4 15 16 25
$\langle \sigma_1 \rangle$	1 24 23 12 11 2 3 6 7 10 13 14 15 22 21 16 9 8 17 18 5 4 19 20 25
$\langle \sigma_1 \sigma_2 \rangle$, (a)	1 24 23 18 17 2 3 10 11 16 19 20 15 12 9 4 5 8 13 14 21 22 7 6 25
$\langle \sigma_1 \sigma_2 \rangle$, (b)	1 24 23 18 17 2 3 14 13 4 5 8 9 12 15 16 19 20 11 10 21 22 7 6 25
$\{id\}$	1 24 23 18 17 2 3 6 7 16 19 20 15 8 9 14 21 22 13 10 5 4 11 12 25

Table 4.3: Sturm permutations π with the filled plane hexahedral (cube) graph as connection graph and adjacent extrema $\underline{v}$, $\bar{v}$. Substitution equivalent and orientation isomorphic copies are omitted. See also figure 4.7.

Isotropy I	Sturm Permutation
$\langle \sigma_2 \rangle$	1 16 17 24 23 18 15 8 9 14 19 20 13 10 7 2 3 6 11 12 21 22 5 4 25
$\langle \sigma_1 \sigma_2 \rangle$, (a)	1 16 17 24 23 18 15 4 5 14 19 20 13 6 7 12 21 22 11 8 3 2 9 10 25
$\langle \sigma_1 \sigma_2 \rangle$, (b)	1 6 7 24 23 8 9 14 15 22 21 16 13 10 5 4 11 12 17 18 3 2 19 20 25
$\{id\}$, (a)	1 10 11 24 23 12 9 4 5 8 13 14 15 22 21 16 7 6 17 18 3 2 19 20 25
$\{id\}$, (b)	1 16 17 24 23 18 15 12 11 2 3 6 7 10 13 14 19 20 9 8 21 22 5 4 25

Table 4.4: Sturm permutations π with the filled plane hexahedral (cube) graph as connection graph and diagonally opposite extrema $\underline{v}$, $\bar{v}$. Substitution equivalent and orientation isomorphic copies are omitted. See also figure 4.10.

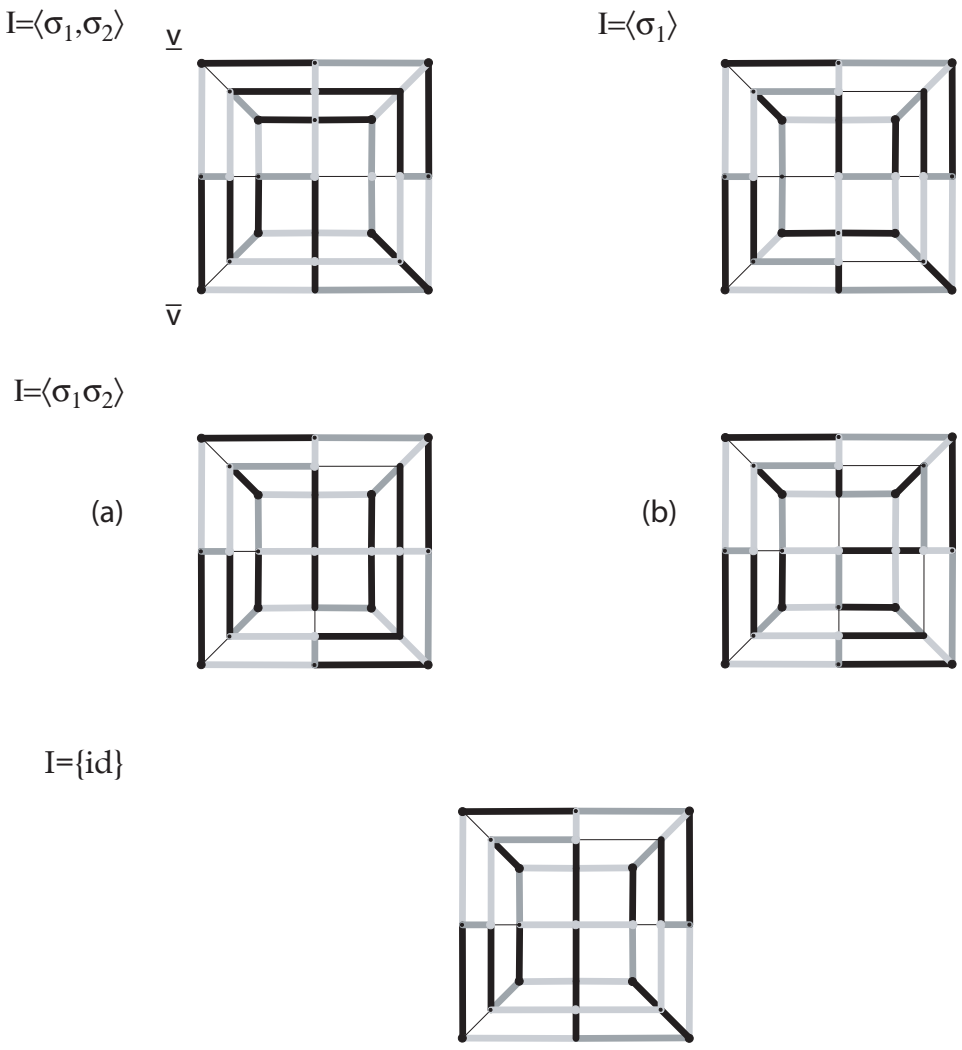

Figure 4.7: The five boundary ZS-Hamiltonian pairs (h_0, h_1) for the planar hexahedral (cube) graph with adjacent extrema $\underline{v}$, $\bar{v}$. For Sturm permutations and enumeration of cases by isotropy I see table 4.3. Edges traversed by both h_0 and h_1 are gray; black is for h_0, light gray for h_1 alone; thin edges for neither.

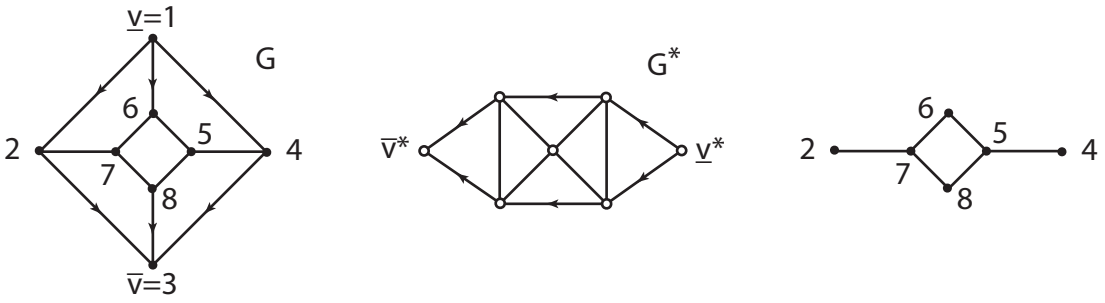

Figure 4.8: The plane hexahedral graph G with diagonally opposite extrema $\underline{v} = 1$, $\bar{v} = 3$. Left: numbering of vertices and basic orientations. Center: the dual 1-skeleton G^*. Right: the central winged square 267854 of G.

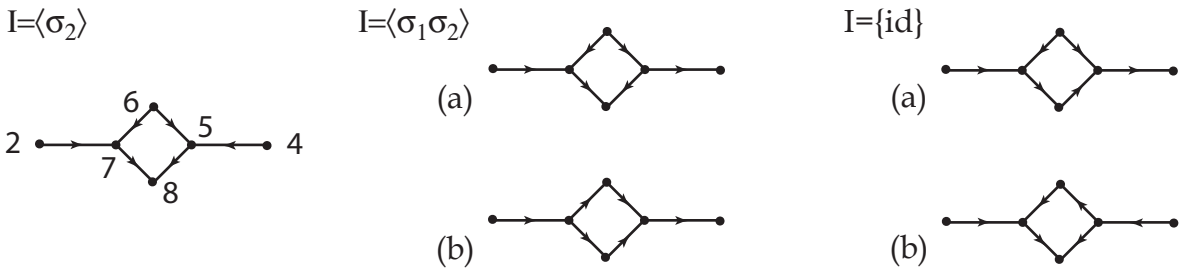

Figure 4.9: Orientations and isotropies of the hexahedral winged squared 267854.

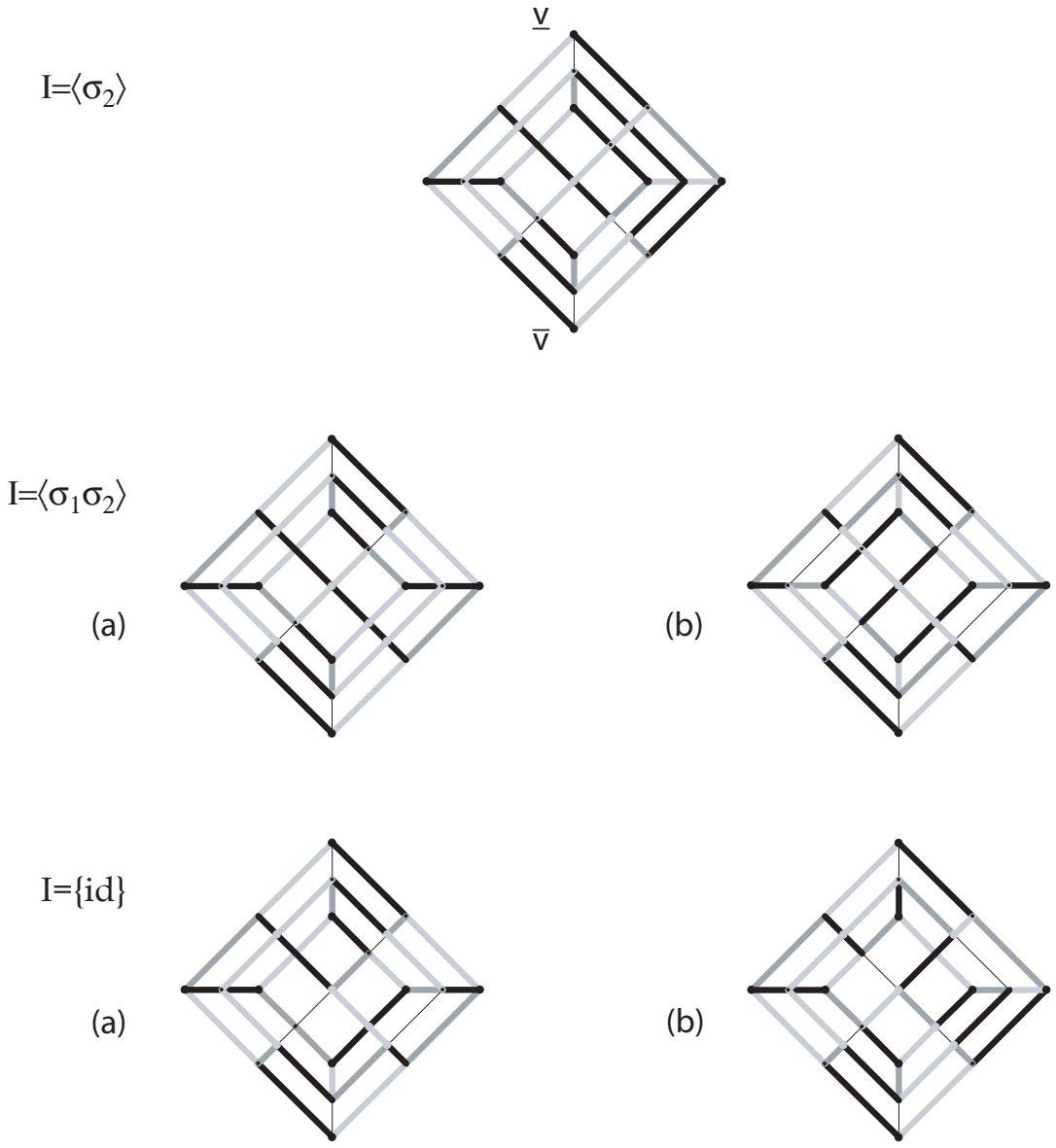

Figure 4.10: The five boundary ZS-Hamiltonian pairs (h_0, h_1) for the planar hexahedral (cube) graph with diagonally opposite extrema $\underline{v}$, $\bar{v}$. For Sturm permutations and enumeration of cases by isotropy I see table 4.4. Edges traversed by both h_0 and h_1 are gray; black is for h_0, light gray for h_1 alone; thin edges for neither.

4.3.1 The case of adjacent extrema $\underline{v}$, $\bar{v}$

Without loss of generality, $\underline{v} = 1$ and $\bar{v} = 2$. See figure 4.5 for the dual 1-skeleton G^*, and for the reduced 1-skeleton $\tilde{G}$ after removal of the trivially glued trapezoid face 1276. Face gluing forces the orientation 67 of the edge {6,7}. Analogously to section 4.2, we perform an admissibility check on the 2^5 orientations of the remaining "letter I" spanned by the vertices 345678. We consider reflections σ_1, σ_2 as before: the axis of σ_2 runs through 1582, vertically, whereas σ_1 bisects the edges 43, $\{5, 8\}$ and 67 horizontally. Di-criticality and acyclicity constraints on admissible orientations lead to the five cases listed in figure 4.6. We leave the derivation, which is analogous to section 4.2, to our reader as an exercise.
For boundary ZS-Hamiltonian pairs from $\underline{v} = 1$ to $\bar{v} = 2$ generated by these orientations see figure 4.7. In table 4.3 we list the resulting five Sturm permutations. Again, we omit σ_1-related cases, alias $\kappa\pi^{-1}\kappa$. Only for trivial isotropy, the remaining σ_2-related case has to be added. Only the cases with isotropy $I = \langle\sigma_1, \sigma_2\rangle$ and $I = \langle\sigma_1\rangle$ are pitchforkable.

4.3.2 The case of diagonally opposite extrema $\underline{v}$, $\bar{v}$

Without loss of generality, $\underline{v} = 1$ and $\bar{v} = 3$. See figure 4.8 for G^* to see that G is neither face-glued nor stacked. This leaves us with 2^6 orientations for the central winged square 267854 to check for admissibility.
Analogously to figures 4.3 and 4.6 we arrive at the five admissible orientations of figure 4.9, listed by decreasing isotropy with respect to the horizontal and vertical reflections σ_1, σ_2 of the winged square.
In addition to σ_1, this time, also σ_2 acts on the non-reduced 1-skeleton G itself, by interchange of the paths h_0 and h_1. Since relabeling of vertices does not affect the Sturm permutation π, this amounts to the trivial substitution equivalence $\pi \leftrightarrow \pi^{-1}$. Therefore only five cases arise, up to trivial substitutions. See table 4.4 and figure 4.10. None of the resulting cases is pitchforkable.

4.4 The plane dodecahedral graph

The plane dodecahedral graph G, as a 1-skeleton, features 30 edges. Since ∂G is a 5-gon, and by the rotation and reflection symmetries of the dodecahedron, it is sufficient to consider two relative positions of the extrema $\underline{v}$, $\bar{v}$ on ∂G: adjacent, or else at distance 2. Either case fixes the orientations of the five boundary edges. In the adjacent case, moreover, the 5-gon containing $\underline{v}$, $\bar{v}$ also fixes the orientations of an additional 4 interior edges. As for the cube in section 4.3.1, this follows because the dual 1-skeleton G^* is then stacked, the face adjacent to $\underline{v}$ and $\bar{v}$ is trivially face glued, and the boundary orientation of theorem 1.1 applies to

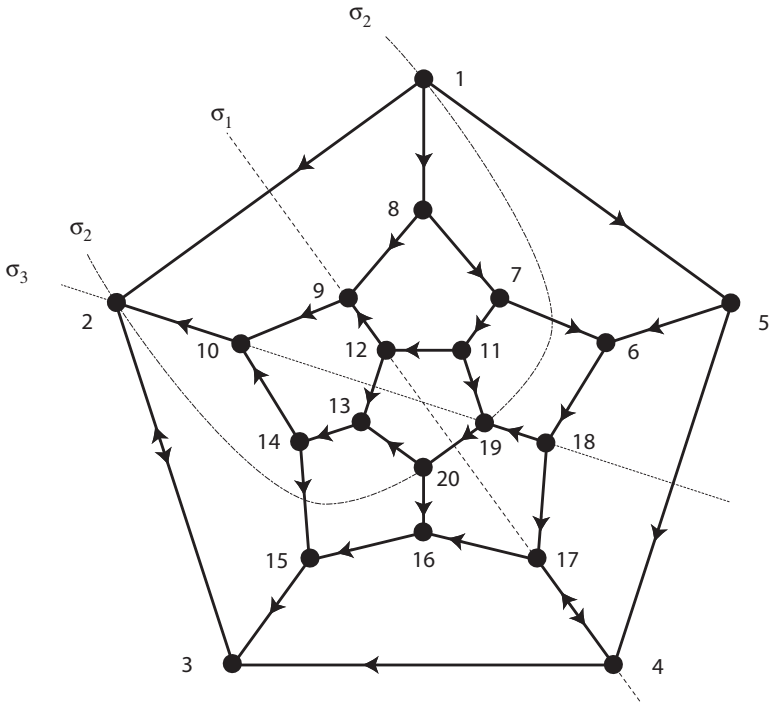

Figure 4.11: Orientations and symmetries of the plane dodecahedron.

G^*. In any case, we are left with 2^{21} possibilities to discuss for an orientation of G, many of which are admissible. The group generated by the symmetries σ_1, σ_2, as in the previous sections, will be of little help in any attempt of a complete enumeration. With a merciful eye on the referee, and ourselves, we only discuss three examples which differ by flipping the orientation of only two edges, as indicated in figure 4.11.
Our examples differ in the orientation of the edges {2,3} and {4,17}. We distinguish the three cases of table 4.5. In cases 1 and 2 the extrema $\underline{v}$, $\bar{v}$ are adjacent in G. After removal of the glued face 1 8 9 10 2 we obtain the reflection symmetries σ_1, σ_2 of the reduced 1-skeleton $\tilde{G}$, as in the previous sections and as indicated in figure 4.11. This time, however, the edges {9,12} and {4,17} come to lie on the reflection axis of σ_1. Since σ_1 reverses orientations, this implies that σ_1 cannot be in the isotropy of any orientation. Likewise, σ_2 cannot be an isotropy element because the axis of σ_2 bisects the edges {6,7} and {14,15}, but does not reverse orientations. Therefore, the maximal isotropy of any admissible orientation is $I = \langle \sigma_1 \sigma_2 \rangle$, as exemplified in case 1. Reversing only the orientation of the edge {4,17}, as in case 2, is sufficient to eliminate all isotropy. Case 3, finally, moves the extremum $\bar{v}$ from 2

Case	{2,3}	{4,17}	$\underline{v}$	$\bar{v}$	isotropy I
1	$3 \to 2$	$4 \to 17$	1	2	$\langle \sigma_1 \sigma_2 \rangle$
2	$3 \to 2$	$17 \to 4$	1	2	$\{id\}$
3	$2 \to 3$	$4 \to 17$	1	3	$\{id\}$

Table 4.5: Three examples of orientations of the plane dodecahedron, distinguished by orientations of the edges {2,3} and {4,17}. See also figure 4.11.

Case	Sturm Permutation
1	1 60 59 12 13 54 53 14 15 26 27 38 29 52 55 56 51 40 37 28 25 16 11 2 3 10 17 18 19 24 29 30 31 36 41 42 43 50 57 58 49 44 35 32 23 20 9 4 5 8 21 22 33 34 45 46 7 6 47 48 61
2	1 60 59 8 9 54 53 10 11 26 27 38 39 52 55 56 51 40 37 28 25 12 7 2 3 6 13 14 15 24 29 30 31 36 41 42 43 50 57 58 49 44 35 32 23 16 17 22 33 34 45 46 21 18 5 4 19 20 47 48 61
3	1 58 57 12 13 52 51 14 15 26 27 38 39 50 53 54 49 40 37 28 25 16 11 2 3 10 17 18 19 24 29 30 31 36 41 42 43 48 55 56 59 60 47 44 35 32 23 20 9 4 5 8 21 22 33 34 45 46 7 6 61

Table 4.6: Three Sturm permutations of dodecahedra. For enumeration of cases by isotropy I see table 4.5 and figure 4.12.

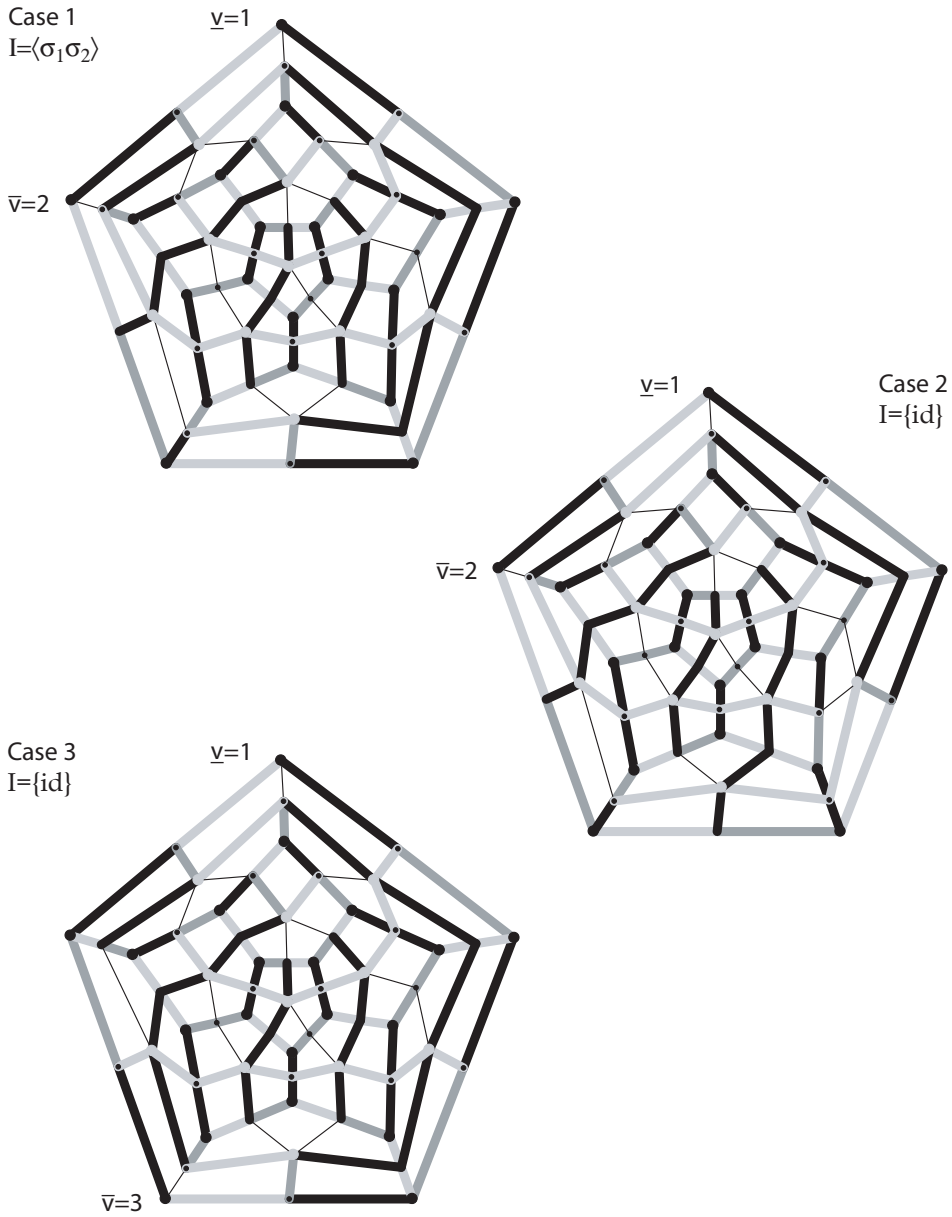

Figure 4.12: Boundary ZS-Hamiltonian paths h_0, h_1 for the three dodecahedral orientations of table 4.5. Edges traversed by both h_0 and h_1 are gray; black is for h_0, light gray for h_1 alone; thin edges for neither.

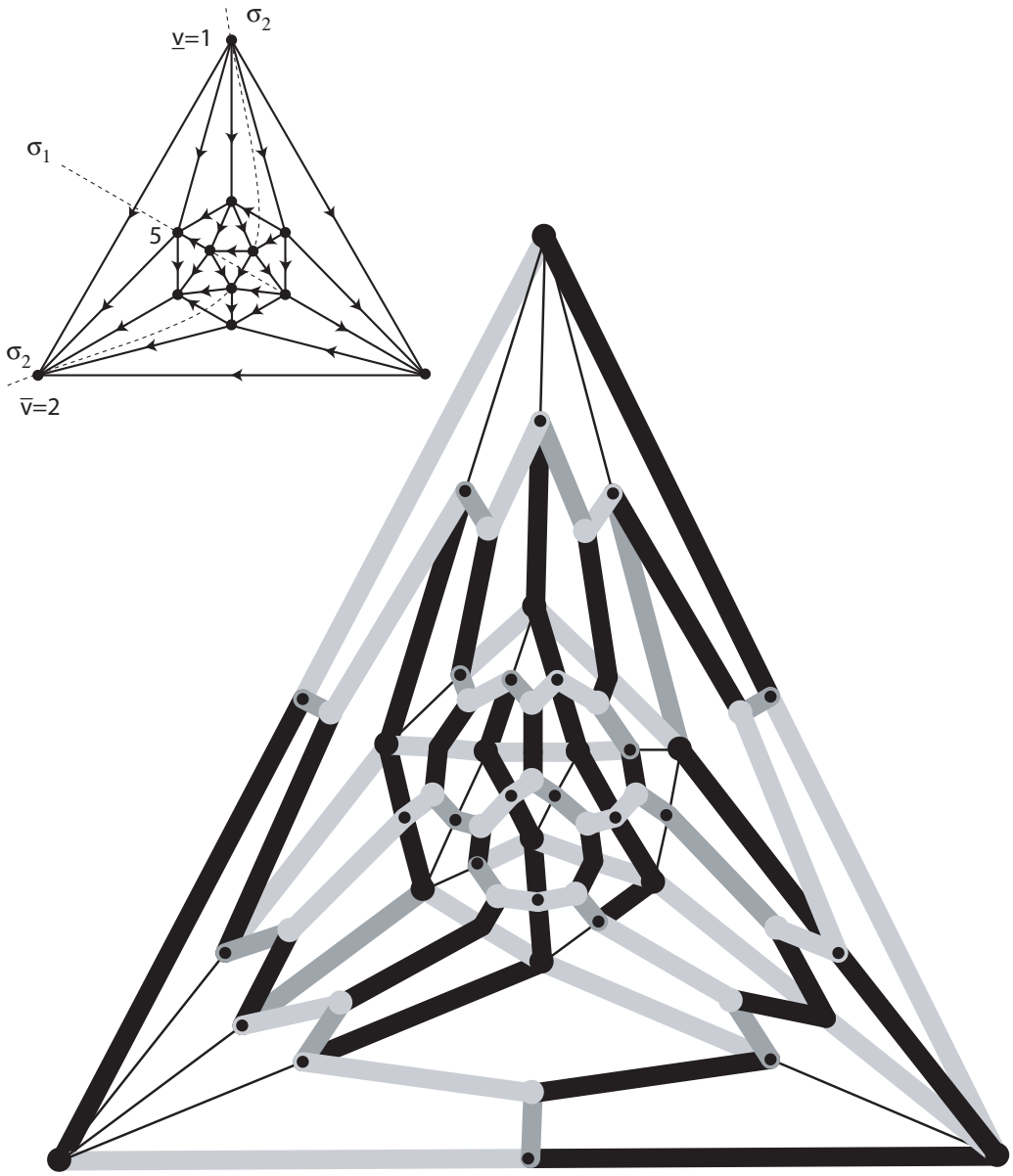

Figure 4.13: An example of the plane icosahedron. Insert: orientations and symmetries. Main: boundary ZS-Hamiltonian paths h_0, h_1. Edges traversed by both h_0 and h_1 are gray; black is for h_0, light gray for h_1 alone; thin edges for neither.

to 3. This leaves only the reflection σ_3 as a candidate for isotropy. However, σ_3 fails because it reverses orientation and contains the edges {2,10} and {18,19} of the 1-skeleton.
The ZS-Hamiltonian pairs (h_0, h_1) for all three cases are illustrated in figure 4.12. Note the invariance of paths and the reversal of orientations in $\tilde{G}$ effected by the isotropy $\sigma_1\sigma_2$ in case 1. Also note how the "atomic" orientation flips from case 1 to cases 2 and 3, respectively, are accommodated by rather localized changes in the Hamiltonian paths. The resulting changes in the Sturm permutations $\pi = h_0^{-1}h_1$, however, are quite nonlocal; see table 4.6. All three cases are pitchforkable.

4.5 The plane icosahedral graph

As a final illustration of design of Sturm attractors we consider the plane icosahedral 1-skeleton G, again with 30 edges. The extrema $\underline{v}$, $\bar{v}$ are necessarily adjacent on the triangular boundary; see the insert of figure 4.13. The face 125 is therefore glued. The reduced 1-skeleton $\tilde{G}$ possesses the indicated symmetries σ_1 and σ_2, as discussed in the sections above. For the same reasons as in section 4.4, neither σ_1 nor σ_2 alone can be an isotropy element. Since we are left with 2^{21} choices for the remaining edge orientations, once again many of them admissible, we select a single example orientation with isotropy $I = \langle\sigma_1\sigma_2\rangle$. See figure 4.13 for the chosen orientation of the 1-skeleton G and for the resulting ZS-Hamiltonian paths h_0 and h_1. Note grayscale preservation and orientation reversal under the rotation $\sigma_1\sigma_2$, outside the glued on triangle 125. The Sturm permutation $\pi = h_0^{-1}h_1$ of this example is multiply pitchforkable:

$$
\begin{aligned}
\pi \;=\; & (1\ 60\ 59\ 52\ 51\ 20\ 19\ 4\ 5\ 18\ 21\ 50\ 49\ 34\ 33\ 22\ 17\ 16\ 23\ 32 \\
& 35\ 48\ 53\ 58\ 57\ 54\ 47\ 46\ 45\ 36\ 31\ 30\ 29\ 24\ 15\ 14\ 13\ 6\ 3\ 2 \\
& 7\ 12\ 25\ 28\ 37\ 44\ 43\ 38\ 27\ 26\ 11\ 10\ 39\ 42\ 55\ 56\ 41\ 40\ 9\ 8\ 61)
\end{aligned}
\tag{4.1}
$$

References

[An86] S. Angenent. The Morse-Smale property for a semi-linear parabolic equation. *J. Diff. Eqns.* **62** (1986), 427–442.

[An88] S. Angenent. The zero set of a solution of a parabolic equation. *Crelle J. reine angew. Math.*, **390** (1988), 79–96.

[ArVi89] V.I. Arnol'd and M.I. Vishik et al. Some solved and unsolved problems in the theory of differential equations and mathematical physics. *Russian Math. Surveys* **44** (1989), 157–171.

[BaVi92] A.V. Babin and M.I. Vishik. *Attractors of Evolution Equations.* North Holland, Amsterdam, 1992.

[BeWi97] L.W. Beineke and R.J. Wilson (eds.). *Graph Connections. Relationships between Graph Theory and other Areas of Mathematics.* Clarendon Press, Oxford, 1997.

[Br90] P. Brunovský. The attracor of the scalar reaction diffusion equation is a smooth graph. *J. Dynamics and Differential Equations*, **2** (1990), 293–323.

[BrFi86] P. Brunovský and B. Fiedler. Numbers of zeros on invariant manifolds in reaction-diffusion equations. *Nonlinear Analysis, TMA* **10** (1986), 179–193.

[BrFi88] P. Brunovský and B. Fiedler. Connecting orbits in scalar reaction diffusion equations. *Dynamics Reported* **1** (1988), 57–89.

[BrFi89] P. Brunovský and B. Fiedler. Connecting orbits in scalar reaction diffusion equations II: The complete solution. *J. Diff. Eqns.* **81** (1989), 106–135.

[ChIn74] N. Chafee and E.F. Infante. A bifurcation problem for a nonlinear partial differential equation of parabolic type. *Appl. Analysis* **4** (1974), 17–37.

[ChVi02] V.V. Chepyzhov and M.I. Vishik. *Attractors for Equations of Mathematical Physics.* Colloq. AMS, Providence, 2002.

[CoSm83] C.C. Conley and J. Smoller. Algebraic and topological invariants for reaction-diffusion equations. In *Systems of Nonlinear Partial Differential Equations*, Proc. NATO Adv. Study Inst., Oxford/U.K. 1982, *NATO ASI Ser. C* **111** (1983), 3-24.

[Ed&al94] A. Eden, C. Foias, B. Nicolaenko, R. Temam. *Exponential Attractors for Dissipative Evolution Equations.* Wiley, Chichester 1994.

[Fi94] B. Fiedler. Global attractors of one-dimensional parabolic equations: sixteen examples. *Tatra Mountains Math. Publ.*, **4** (1994), 67–92.

[Fi02] B. Fiedler (ed.) *Handbook of Dynamical Systems* **2**, Elsevier, Amsterdam 2002.

[FiRo96] B. Fiedler and C. Rocha. Heteroclinic orbits of semilinear parabolic equations. *J. Diff. Eq.* **125** (1996), 239–281.

[FiRo99] B. Fiedler and C. Rocha. Realization of meander permutations by boundary value problems. *J. Diff. Eqns.* **156** (1999), 282–308.

[FiRo00] B. Fiedler and C. Rocha. Orbit equivalence of global attractors of semilinear parabolic differential equations. *Trans. Amer. Math. Soc.* **352** (2000), 257–284.

[FiRo07a] B. Fiedler and C. Rocha. Connectivity and design of planar global attractors of Sturm type. I: Orientations and Hamiltonian paths. Submitted 2007.

[FiRo07b] B. Fiedler and C. Rocha. Connectivity and design of planar global attractors of Sturm type. II: Connection graphs. Submitted 2007.

[FiSche03] B. Fiedler, A. Scheel. Spatio-temporal dynamics of reaction-diffusion patterns. In *Trends in Nonlinear Analysis*, M. Kirkilionis et al. (eds.), Springer-Verlag, Berlin 2003, 23–152.

[FuRo91] G. Fusco and C. Rocha. A permutation related to the dynamics of a scalar parabolic PDE. *J. Diff. Eqns.* **91** (1991), 75–94.

[Ga04] V.A. Galaktionov. *Geometric Sturmian Theory of Nonlinear Parabolic Equations and Applications.* Chapman & Hall, Boca Raton 2004.

[Ha88] J.K. Hale. *Asymptotic Behavior of Dissipative Systems*. Math. Surv. **25**. AMS Publications, Providence 1988.

[Ha&al02] J.K. Hale, L.T. Magalhães, and W.M. Oliva. *Dynamics in Infinite Dimensions.* Springer-Verlag, New York 2002.

[HaMi91] H. Hattori and K. Mischaikow. A dynamical system approach to a phase transition problem. *J. Diff. Eqns.* **94** (1991), 340–378.

[He81] D. Henry. *Geometric Theory of Semilinear Parabolic Equations*. Lect. Notes Math. **804**, Springer-Verlag, New York 1981.

[He85] D. Henry. Some infinite dimensional Morse-Smale systems defined by parabolic differential equations. *J. Diff. Eqns.* **59** (1985), 165–205.

[La91] O.A. Ladyzhenskaya. *Attractors for Semigroups and Evolution Equations*. Cambridge University Press, 1991.

[Ma78] H. Matano. Convergence of solutions of one-dimensional semilinear parabolic equations. *J. Math. Kyoto Univ.* **18** (1978), 221–227.

[Ma82] H. Matano. Nonincrease of the lap-number of a solution for a one-dimensional semilinear parabolic equation. *J. Fac. Sci. Univ. Tokyo Sec. IA*, **29**(1982), 401–441.

[Ma88] H. Matano. Asymptotic behavior of solutions of semilinear heat equations on S^1. In *Nonlinear Diffusion Equations and their Equilibrium States II* . W.-M. Ni, L.A. Peletier, J. Serrin (eds.). 139–162. Springer-Verlag, New York, 1988.

[MaNa97] H. Matano and K.-I. Nakamura. The global attractor of semilinear parabolic equations on S^1. *Discr. Contin. Dyn. Syst.* **3** (1997), 1–24.

[PdM82] J. Palis and W. de Melo. *Geometric Theory of Dynamical Systems. An Introduction.* Springer-Verlag, New York, 1982.

[Pa83] A. Pazy. *Semigroups of Linear Operators and Applications to Partial Differential Equations*. Springer-Verlag, New York, 1983.

[Ra02] G. Raugel. Global attractors. In [Fi02], 885–982, 2002.

[Ro91] C. Rocha. Properties of the attractor of a scalar parabolic PDE. *J. Dyn. Diff. Eqns.* **3** (1991), 575–591.

[SeYo02] G.R. Sell, Y. You. *Dynamics of Evolutionary Equations.* Springer-Verlag, New York 2002.

[St1836] C. Sturm. Sur une classe d'équations à différences partielles. *J. Math. Pure Appl.* **1** (1836), 373–444,.

[Ta79] H. Tanabe. *Equations of Evolution*. Pitman, Boston, 1979.

[Te88] R. Temam. *Infinite-Dimensional Dynamical Systems in Mechanics and Physics*. Springer-Verlag, New York, 1988.

[Wo02a] M. Wolfrum. A sequence of order relations: Encoding heteroclinic connections in scalar parabolic PDE. *J. Diff. Eqns.* **183** (2002), 56–78.

[Wo02b] M. Wolfrum. Geometry of heteroclinic cascades in scalar parabolic differential equations. *J. Dyn. Differ. Equations* **14** (2002), 207–241.

[Ze68] T.I. Zelenyak. Stabilization of solutions of boundary value problems for a second order parabolic equation with one space variable. *Diff. Eqns.* **4** (1968), 17–22.